Control System Performance of a Woofer-Tweeter Adaptive Optics System

Colin Bradley, Rodolphe Conan
Department of Mechanical Engineering, University of Victoria
Peter J. Hampton, Pan Agathoklis
Department of Electrical and Computer Engineering, University of Victoria

ABSTRACT

This paper describes the control of two deformable mirrors (DM) and a tip tilt mirror for adaptive optics. The purpose of this experimental adaptive optics system at the University of Victoria is to prove the Woofer Tweeter concept for use in instruments for the Thirty Meter Telescope (TMT) that is currently under development. The first deformable mirror is a large stroke DM (Woofer) capable of lower frequency correction in both the temporal and spatial domains. The other DM (Tweeter) is capable of the high temporal and spatial frequency corrections of the turbulence. The response speed of the Woofer is incorporated into the Tweeter controller in order to allow for appropriate offloading from the Tweeter to the Woofer. In order to determine which Tweeter shapes should be compensated for the slower Woofer and which are not coupled to the Woofer, the cross correlation of the devices is determined. The method of converting the wave front sensor (WFS) measurements to control signal error is given. The transfer functions of the controller are provided, along with rejection ratio plots, bandwidths and amplitude response to system noise.

1. INTRODUCTION

A simple adaptive optics system for astronomy uses a single wave front sensor (WFS) and a single deformable mirror (DM) to correct for the distortions imposed on light by the atmosphere and the static aberrations of the telescope optics [1]. In the next generation telescopes, both the actuator density and maximum actuator stroke requirements increase significantly due to the enormity of these very large telescopes. Current technology is cost prohibitive to design a single mirror that satisfies both of these requirements. Fortunately, the large stroke required is for the compensation of low spatial frequency distortions [2]. This allows the system to be designed with two DMs; (i) a high stroke, low actuator density DM named the Woofer and (ii) a low stroke, high actuator density DM named the Tweeter. The Woofer for this test bench was produced by the Laboratory of Astrophysics of the Observatory of Grenoble (LAOG) and has 52 actuators on an 8x8 grid. The Tweeter was produced by Boston Micromachines Corporation and has 140 actuators on a 12x12 grid. The Adaptive Optics Laboratory at the University of Victoria has recently produced a test bench for this Woofer-Tweeter system. This project is part of the development of the Thirty Meter Telescope (TMT) that will be built in the next decade.

Initial simulated and experimental results have shown that the developed controller can appropriately split the correction between the mirrors and acts similarly to the single DM case [3]. The Woofer corrects for the low-spatial-low-temporal frequency disturbances and the Tweeter corrects for the remaining disturbance. It has been assumed that the Woofer can respond slower than the tweeter. The Woofer's impulse response is modeled as an exponential decay given by $e^{kT_s/\tau}$. A one dimensional representation of the controller approach is shown in Fig. 1. The Woofer slowly approaches the steady state of the input signal. During this time, the Tweeter compensates for the residual error. The combined response of the two DMs is then equal to how the single DM case would respond to the input. A simple layout of the single DM system components is shown in Figure 4. This paper focuses primarily on discrete control in the Z-domain [4].

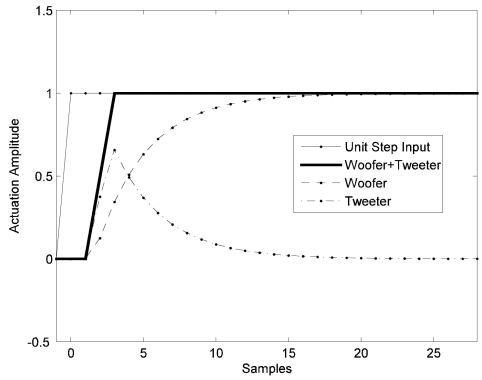

Fig. 1. One-dimensional mode off-loading example.

2. WOOFER-TWEETER MODE SELECTION

A straight forward approach to controlling this Woofer-Tweeter system would be to simply do a global interaction matrix and control the entire system as a single device as in Eq. 2.1. Although conceptually simple and shown to work in simulations, this method proved difficult, if not impossible to use in practice. It is believed that a strong reason for this is that the ratio of actuator motion to control signal for the Woofer is on the order of 1000 times that of the Tweeter. So any measurement noise on the Woofer portion of the interaction matrix would be 1000 times larger than the noise on the Tweeter portion. This could make the Woofer noise significant compared with the Tweeter portion of the global interaction matrix.

$$D_{Global} = \begin{bmatrix} D_{tt} & D_{wr} & D_{tr} \end{bmatrix} \tag{2.1}$$

Where D will represent the interaction matrix and the subscripts tt, wr, tr refer to the Tip Tilt, Woofer and Tweeter mirrors respectively. D^{+} represents the pseudo inverse of the interaction matrix (i.e. the reconstructor matrix).

An alternative approach was developed that treats the mirrors as separate devices. The applicable shapes from one mirror can be offloaded to another in order to reduce the stroke requirements of smaller devices. In order to offload shapes from one mirror to another, the shapes that are correlated between the mirrors must be determined. The first step is to find the separate interaction matrix for each individual mirror (D_{tt}, D_{wr} and D_{tr}). Zonal interaction matrices were chosen for this experiment.

2.1. Actuator Linearization

Before shapes can accurately be transferred between mirrors, the mirrors need to be linear, otherwise simple addition and subtraction does not apply. Fortunately the response of the Woofer actuators was found to already be linear in the necessary range of motion. However, the MEMS Tweeter has a quadratic response. This was measured by moving the given actuator to 8 different positions and measuring the respective actuator error using the initial Tweeter reconstructor matrix (D_{tr}^{+}). Then a quadratic function is fit to these 8 data points to determine the coefficients (a, b and c) in a least squares sense using a Vandermonde matrix.

$$f(x) = ax^2 + bx + c \tag{2.2}$$

The values of $f(x)$ are somewhat arbitrary because the reconstructor used was made using a non-linear Tweeter. They are also relative to the position that happens to cause 0 error. Once the coefficients are found, c is set to 0 so that when $x = 0$, $f(x)$ will also equal 0. The output to the Tweeter is then found by Eq. 2.3. The sign of the square route has the same sign as b. Once this linearization is complete, D_{tr} must be re-evaluated using the linear actuator response.

$$x = \frac{-b \pm \sqrt{b^2 + 4ay}}{2a} \tag{2.3}$$

where y is the desired actuation of the tweeter actuator
x is the output to the tweeter

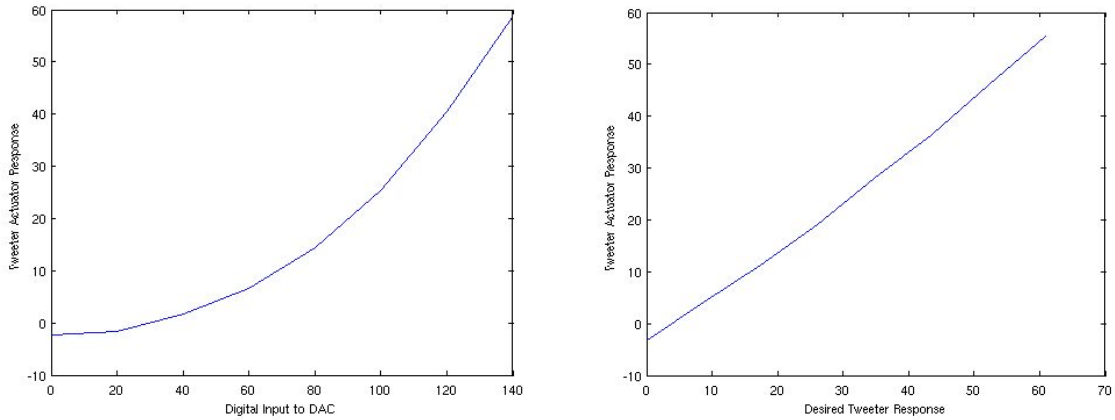

Fig. 2. Quadratic actuator response of the Tweeter (left) and linear response when applying Eq. 2.3 (right).

2.2. Tip Tilt Correlation

A goal of the project is to offload the average tilt to a tilt mirror or a tilt mount that can tilt a DM. This would be offloading at a very slow rate and would probably not occur each sample. In the mean time, there is full offloading to the tip tilt mirror and the Woofer and Tweeter do not perform any tilt correction. This is accomplished by first determining what shapes are correlated between each DM and the Tip Tilt mirror by taking advantage of Singular Value Decomposition (SVD) [5]. Since D_{tt} is two vectors, there are only 2 non-zero singular values and the first 2 column vectors of $U_{<tr,tt>}$ will each be a set of Tweeter actuator commands that is the best fit to one of the two tilts. The same is repeated for the Woofer.

$$U_{<tr,tt>}W_{<tr,tt>}V^T_{<tr,tt>} = D^+_{tr}D_{tt} \tag{2.4}$$

$$B_{<tr,tt>} = [\vec{u}_{<tr,tt>,1} \quad \vec{u}_{<tr,tt>,2}] \tag{2.5}$$

$$U_{<wr,tt>}W_{<wr,tt>}V^T_{<wr,tt>} = D^+_{wr}D_{tt} \tag{2.6}$$

$$B_{<wr,tt>} = [\vec{u}_{<wr,tt>,1} \quad \vec{u}_{<wr,tt>,2}] \tag{2.7}$$

where < , > denotes correlation of two mirrors.
B is a subset of orthogonal mirror shapes
$\vec{u}_k$ is the kth column vector of U

2.3. Woofer-Tweeter Correlation

The correlation between the Woofer and the Tweeter is conducted in a similar way. The difference is that the correlated shapes with the Tip Tilt mirror must be suppressed. Again, this can be achieved by taking advantage of the SVD.

$$U_{<tr,wr>}W_{<tr,wr>}V^T_{<tr,wr>} = \left(I - B_{<tr,tt>}B^T_{<tr,tt>}\right)D^+_{tr}D_{wr}\left(I - B_{<wr,tt>}B^T_{<wr,tt>}\right) \tag{2.8}$$

where $B_{<tr,wr>} = [\vec{u}_{<tr,wr>,1} \quad \vec{u}_{<tr,wr>,2} \quad \cdots \quad \vec{u}_{<tr,wr>,N}]$

$B_{<wr,tr>} = [\vec{v}_{<tr,wr>,1} \quad \vec{v}_{<tr,wr>,2} \quad \cdots \quad \vec{v}_{<tr,wr>,N}]$

$\left(I - B_{<wr,tt>}B^T_{<wr,tt>}\right)B_{<wr,tt>} = null$

$B^T_{<tr,tt>}\left(I - B_{<tr,tt>}B^T_{<tr,tt>}\right) = null$

N is the number of chosen correlated Woofer Tweeter modes

The matrix $V_{<tr,wr>}$ is a matrix of Woofer shapes that match the Tweeter shapes in matrix $U_{<tr,wr>}$. The match is made in WFS space and so is only dependant on the calibration data and does not require additional modeling. They are ordered left to right from highest correlation to least. All singular values beyond the N number cut off should be forced to 0. The shapes that are correlated with the Tip Tilt mirror result in a null matrix, so these are assigned the least amount of correlation with the other mirror and these shapes are automatically moved to the end of the set. The result is shown in the following figure. The first 12 shapes that have high correlation between the Woofer and the Tweeter are shown in order from left to right and top to bottom. This figure was generated by applying the modes to a virtual Woofer mirror in MatLab and generating a plot of the phase. The modes are very similar to the Zernike set of modes [2] starting with focus, then astigmatism followed by coma and trefoil and finally some 4th order shapes. The modes are off center and this may be due to a shifted alignment between the Woofer and the Tweeter.

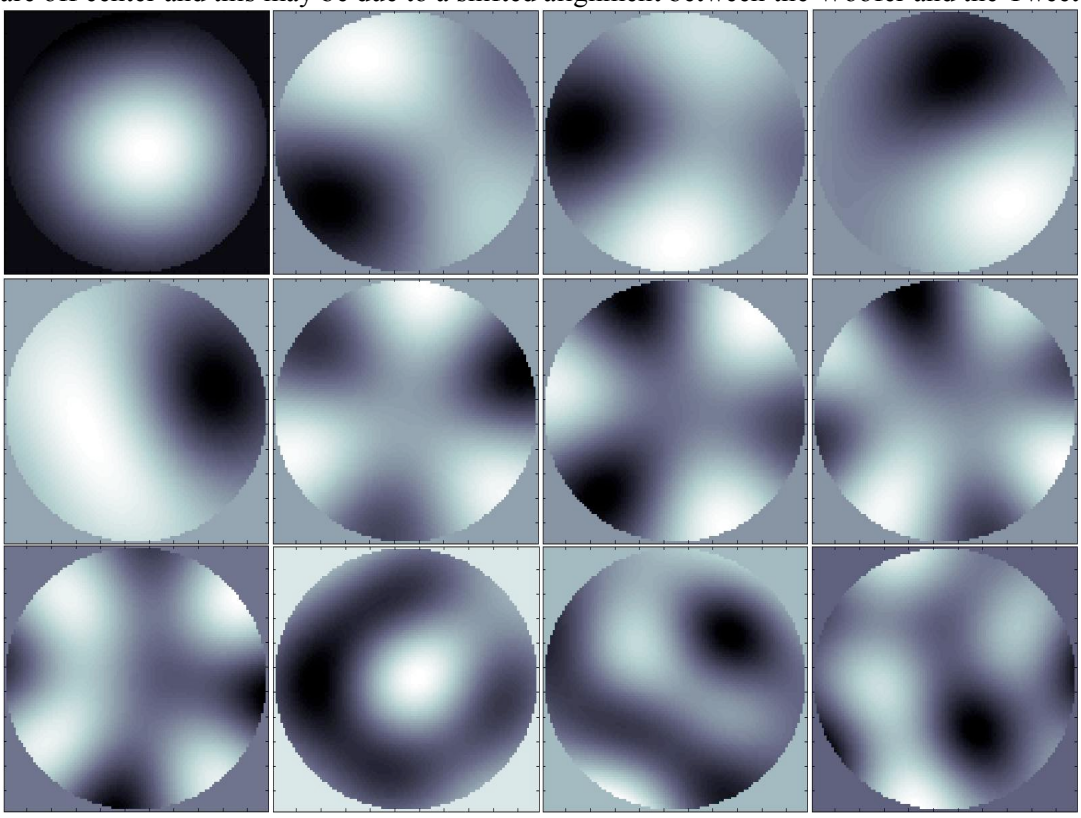

Fig. 3. The first 12 woofer-tweeter modes.

2.4. Reconstructors

The reconstruction of WFS measurements to mirror actuator commands will occur in stages. This allows the WFS error measurement to propagate to the mirrors without the ratio of real actuator motion to control signal being a factor as in the Global Interaction case. The first stage is to convert the measured WFS error to Tweeter actuator error with D_{tr}^{+}. Then Tweeter actuator error is converted to Tip Tilt error using Eq. 2.10 and Woofer error using Eq. 2.11. The controllers that handle these signals are derived in Section 3.

$$E_{tr} = D_{tr}^{+} E_{WFS} \tag{2.9}$$

$$E_{tt} = V_{<tr,tt>} W_{<tr,tt>}^{+} U_{<tr,tt>}^{T} E_{tr} \tag{2.10}$$

$$E_{wr} = V_{<tr,wr>} W_{<tr,wr>}^{+} U_{<tr,wr>}^{T} E_{tr} \tag{2.11}$$

3. CONTROL SYSTEM

3.1. Model of an adaptive optics system

The model of an Adaptive Optics system has been determined by several independent researchers in either the continuous or discrete domains. The common continuous model is one where the WFS is modeled as a zero order hold divided by the sample time. The Laplace transform of a zero order hold is given in Eq. 3.1 and that of the WFS in Eq. 3.2. A zero order hold is also necessary to model the conversion of the sampled data into a pulse with the sample time as its duration. The updating of the DM is modeled as a delay, which can be a fraction of the sample time (Eq. 3.3).

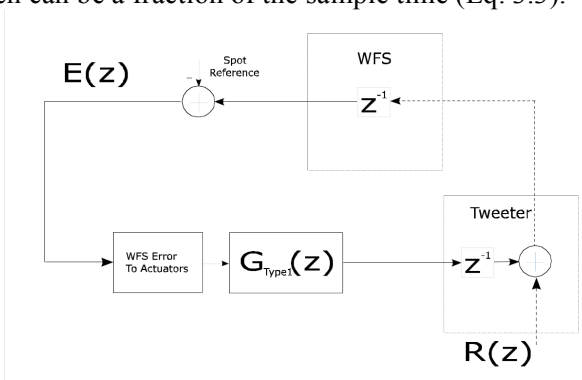

Fig. 4. Discrete model of a single mirror AO system.

$$G_{ZOH}(s) = \frac{1 - e^{sT_s}}{s} \tag{3.1}$$

$$G_{WFS}(s) = \frac{1 - e^{sT_s}}{sT_s} \tag{3.2}$$

$$G_{DM}(s) = e^{s\varphi} \tag{3.3}$$

where T_s is the sample time and φ is the delay

The system that is controlled (i.e. the plant) is given as $G_P(s)$ in Eq. 3.5 for the continuous domain and as $G_P(z)$ in Eq. 3.8 for the discrete time model.

$$G_P(s) = G_{DM}(s) G_{WFS}(s) G_{ZOH}(s) \tag{3.4}$$

$$G_P(s) = e^{s\varphi}\left(\frac{1 - e^{sT_s}}{sT_s}\right)\left(\frac{1 - e^{sT_s}}{s}\right) \tag{3.5}$$

The experimental setup built at the University of Victoria is representing this model under the assumption that the DM update delay is considered to be one sample period. When φ is an integer multiple of the sample time, the transformation from the continuous domain to the discrete domain is simplified. The discrete model for the system tested at the University of Victoria is simply two sample delays, Eq. 3.8.

$$G_P(z) = Z\left\{e^{sT_s}\left(\frac{1 - e^{sT_s}}{sT_s}\right)\left(\frac{1 - e^{sT_s}}{s}\right)\right\} \tag{3.6}$$

$$G_P(z) = z^{-1}\left(1 - z^{-1}\right)^2 \frac{T_s z^{-1}}{T_s\left(1 - z^{-1}\right)^2} \tag{3.7}$$

$$G_P(z) = z^{-2} = G_{DM}(z) G_{WFS}(z) \tag{3.8}$$

where $G_{DM}(z) = z^{-1}$ (3.9)

$$G_{WFS}(z) = z^{-1} \tag{3.10}$$

3.2. Single deformable mirror control

The simplest approach to controlling such a system is to use a single integrator and adjust the gain in order to make the system stable. This approach will be referred to as the Classic Adaptive Optics (CAO) controller.

$$G_{CAO}(z) = \frac{g}{1 - z^{-1}} \tag{3.11}$$

where g is a variable gain.

The closed loop transfer function of such a system is

$$T_{CAO}(z) = \frac{G_{CAO}(z)G_P(z)}{1 + G_{CAO}(z)G_P(z)} \tag{3.12}$$

$$T_{CAO}(z) = \frac{gz^{-2}}{1 - z^{-1} + gz^{-2}} \tag{3.13}$$

where $T_{CAO}(z)$ is stable for $0 \le g < 1$

However, the control approach used here is to increase the bandwidth by increasing the complexity of the controller by 1 zero and 2 poles. The open loop transfer function of this controller is

$$G_{Type1}(z) = \frac{g\left(0.5 + 0.5z^{-1}\right)}{1 - 0.5z^{-2} - 0.5z^{-3}} \tag{3.14}$$

The closed loop transfer function of the system with this Type 1 controller is

$$T_{Type1}(z) = \frac{g\left(0.5z^{-2} + 0.5z^{-3}\right)}{1 + (g-1)\left(0.5z^{-2} + 0.5z^{-3}\right)} \tag{3.15}$$

where $T_{Type1}(z)$ is stable for $0 \le g < \sqrt{5}$

The closed-loop system for g = 1 using $G_{Type1}(z)$ has all poles at z = 0 and the system responds as the averaging filter of Eq. 3.16. The step response will settle in two samples after the initial delay. It has been found using simulated and experimental results the CAO controller with g = 0.4 gives a similar performance as the Type 1 controller with g = 1.

$$T_{Type1}(z)\Big|_{g=1} = 0.5z^{-2} + 0.5z^{-3} \tag{3.16}$$

3.3. Slow Woofer, Fast Tweeter

It is assumed that the Tweeter responds the same as in the single DM case. One possibility is that the Woofer mirror will have a slower response time than of the Tweeter. If this effect is not considered for the controller design, the controller would over drive the Woofer and unexpected oscillations may occur.

$$G_{Tweeter}(z) = G_{DM}(z) = z^{-1} \tag{3.17}$$

$$G_{Woofer}(z) = \frac{\left(1 - e^{-T_s/\tau}\right)z^{-1}}{1 - e^{-T_s/\tau}z^{-1}} \tag{3.18}$$

where τ is the time constant of the exponential decay

To avoid such a deterioration of performance, a first order response model is assumed for the Woofer. A filter is then developed for the Tweeter that will allow the Woofer-Tweeter combination to have the same response as a single fast DM. The subscript *HP* denotes that it is a High Pass filter.

$$G_{DM}(z) = G_{HP}(z)G_{Tweeter}(z) + G_{Woofer}(z) \tag{3.19}$$

$$G_{HP}(z) = \frac{G_{DM}(z) - G_{Woofer}(z)}{G_{Tweeter}(z)} \tag{3.20}$$

$$G_{HP}(z) = \frac{e^{-T_s/\tau}\left(1 - z^{-1}\right)}{1 - e^{-T_s/\tau} z^{-1}} \tag{3.21}$$

This high pass filter is applied to all mirror shapes that both the Woofer and Tweeter can produce. It is not applied to Tweeter shapes that the Woofer can not produce. This allows the Tweeter to temporarily correct for a new disturbance until the Woofer has enough time to produce the full correction of the given shape. This high pass filter has a zero at z = 1, which will cancel with the integrator in the controller. If this model is a good approximation of the real system, it is expected that the mirrors will seamlessly transfer low temporal frequency disturbance from the Tweeter to the Woofer.

3.4. Tweeter Controller

Even though the Woofer is assumed to respond slower than the Tweeter, the Woofer will be controlled by the same controller as in the single DM case. This is expected to work if the Tweeter corrects the error that remains because of the slow response of the Woofer. For the shapes that overlap between the Woofer and Tweeter mirrors, the Tweeter will be controlled by the controller, $G_{TL}(z)$, given in Eq. 3.24. The integrator of $G_{Type1}(z)$ is cancelled by the zero at z = 1. The subscript *TL* denotes the Tweeter Low spatial frequency controller.

$$G_{TL}(z) = G_{Type1}(z) G_{HP}(z) \tag{3.22}$$

$$G_{TL}(z) = \frac{g\left(0.5 + 0.5z^{-1}\right)}{1 - 0.5z^{-2} - 0.5z^{-3}} \frac{e^{-T_s/\tau}\left(1 - z^{-1}\right)}{1 - e^{-T_s/\tau} z^{-1}} \tag{3.23}$$

$$G_{TL}(z) = \frac{g e^{-T_s/\tau}\left(0.5 + 0.5z^{-1}\right)}{1 + \left(1 - e^{-T_s/\tau}\right)z^{-1} + \left(0.5 - e^{-T_s/\tau}\right)z^{-2} - 0.5e^{-T_s/\tau} z^{-3}} \tag{3.24}$$

The high spatial frequency shapes can not be controlled by the Woofer. Therefore, for those frequencies, all the corrections must be provided by the Tweeter as though it was the only mirror in the system. So, the controller is the same as in the single mirror case.

$$G_{TH}(z) = G_{Type1}(z) \tag{3.25}$$

4. EXPERIMENTAL RESULTS

4.1. Rejection Ratio

The rejection ratio is the amplitude response of the following error. It is often used in Adaptive Optics to assess the bandwidth of the system. This can be determined using

$$\text{Rejection Ratio} = \left|\frac{E(z)}{R(z)}\right| = \left|1 - T(z)\right| \tag{4.1}$$

where E(z) is the measured error
R(z) is the optical disturbance input
T(z) is the closed loop transfer function

This is usually plotted with a logarithmic scale for the frequency and decibel scale for the amplitude. The frequency of the first point of the plot that crosses the 0dB line (starting at 0 Hz and scanning towards the sample rate) is called the 0dB bandwidth.

4.2. White noise input

The disturbance used in the initial experiments is a known but random set of actuator commands for all mirrors. This ensures that the disturbance is correctable since it is on the same scale as the mirrors. The data collected is plotted as rejection ratio plots. White noise input is desirable for constructing rejection ratio plots because it ensures that there is significant power at all frequencies of the spectrum. The expected rejection ratio when the system is operating well is given as Eq. 4.2. The result shown in Fig. 5 shows that when the Woofer is as fast as the Tweeter, the measured rejection ratio matches the single fast DM model. The 0dB bandwidth of this system is approximately 6.5% of the sample rate for the given gain of 1. The error signal is E(z) and the input signal is R(z).

$$\left|\frac{E(z)}{R(z)}\right| = \left|\frac{1}{1+\left(G_{TL}(z)G_{Tweeter}(z)+G_{Type1}(z)G_{Woofer}(z)\right)G_{WFS}(z)}\right| = \left|1-0.5z^{-2}-0.5z^{-3}\right| \quad (4.2)$$

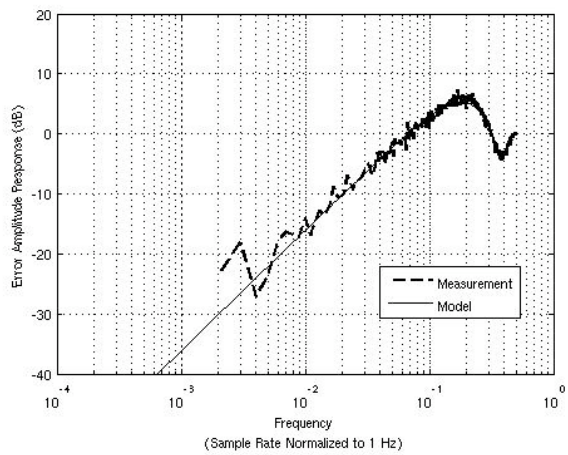

Fig. 5. Rejection ratio of a Woofer mode for $\tau = 0$.

The Woofer was then slowed by filtering the control signals through a first order system. The exponential decay constant, τ, was increased to $20T_s$. This means that the Woofer would settle to within 5% of the steady state output signal in 60 samples. In the mean time, the Tweeter assumes the responsibility for correcting the high frequency component of the Woofer shapes. The result is that the rejection ratio plots for all measured speeds of the Woofer remained consistent with the fast single mirror model. An example of this is given as Fig. 6 (left). This means that the combination of the Tweeter controller and Woofer controller are providing the correct signals to their respective mirrors to achieve the desired correction.

The case when the slow Woofer operates without the aid of the Tweeter was also considered. It is expected that if the Tweeter does not correct for the high frequency disturbance that the rejection ratio would be given by Eq. 4.3. In this case, $\tau = 20T_s$. This model is fully supported by the measurements taken and displayed in Figure 7 (right). It is shown to illustrate the improvement provided by the Tweeter.

$$\left|\frac{E(z)}{R(z)}\right| = \left|\frac{1}{1+G_{Type1}(z)G_{Woofer}(z)G_{WFS}(z)}\right| = \left|\frac{\left(1-0.5z^{-2}-0.5z^{-3}\right)\left(1-e^{-T_s/\tau}z^{-1}\right)}{1-e^{-T_s/\tau}z^{-1}-0.5e^{-T_s/\tau}\left(z^{-2}-z^{-4}\right)}\right| \quad (4.3)$$

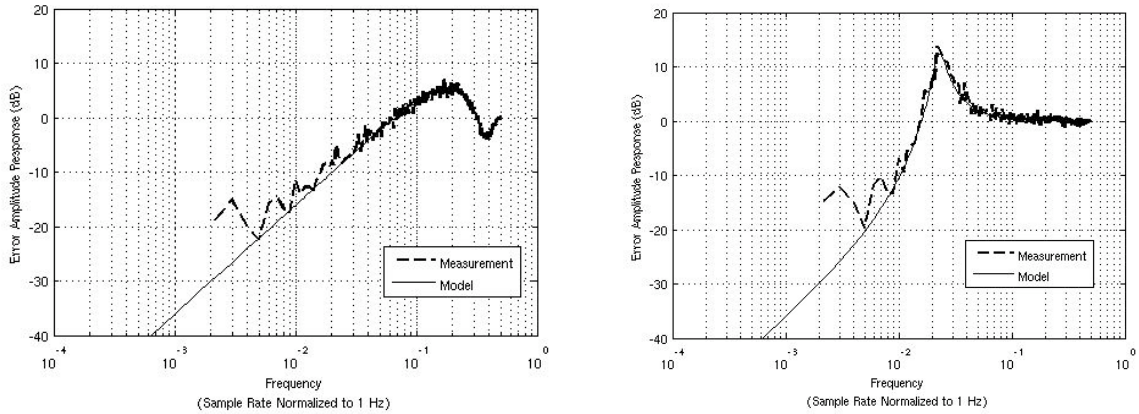

Fig. 6. Rejection ratio of a Woofer mode with (left) and without (right) Tweeter assistance for $\tau = 20T_s$

It was feared that a potential problem for this approach is that the Woofer and Tweeter could form equal but opposite shapes. These distortions on the light beam would cancel with each other before reaching the WFS and be both invisible and a waste of the available stroke of the mirrors. This misbehavior has been avoided in this control scheme by determining the correlated shapes and an offloading the low temporal and spatial frequency modes to the Woofer.

4.3. Simulated turbulence input

Another issue that needed to be studied is the amount of stroke that is offloaded to the Woofer from the Tweeter in this scheme. A simulated phase screen for a turbulence of $D/r_o = 6.25$ was generated and the simulated Tip Tilt mirror and Tweeter corrected it in a simulated AO system. This was to determine appropriate actuator signals that would correspond to such turbulence. These actuator commands were then scaled to generate a significant disturbance and applied to the real Tweeter without the controller's knowledge. Effectively, this generates turbulence that has the correct distribution of spatial and temporal frequency power. It was found that the maximum standard deviation of the Tweeter stroke was 4.859 discrete steps when the maximum standard deviation of the input turbulence was 8.971 discrete steps. The minimum standard deviation of Tweeter actuation was 1.527 discrete steps when the turbulence minimum standard deviation of the turbulence was equivalent to 4.594 discrete steps. So the fast Woofer took almost half of the work, which is similar to the results of the simulation when the Woofer assumed the low order polynomial shapes that were similar to Figure 3. It is important to note that there was no tilt in this input, so a significant amount of offloading to the tilt mirror is not taken into account. Also, since the two mirrors are close to the same dimensions, the correlation between the mirrors is poor after the first 9 or 10 modes. It is expected that when the Tweeter has significantly more actuators than the Woofer that the matching of shapes will be improved and more modes can be offloaded to the Woofer.

5. CONCLUSIONS

The Adaptive Optics test bench at the University of Victoria is used to design and test an Adaptive Optics control system consisting of a slow Woofer mirror and a fast Tweeter mirror. The correlated shapes are determined using WFS measurements from the calibration step. The resultant shapes are similar to low order Zernike modes. Linearization of the Tweeter actuators requires additional computation power but allows linear mathematics to apply for offloading to the Woofer. It also maintains the desired gain value for any level of actuation. Using an appropriate high pass filter in the Tweeter controller provides the necessary offloading of low frequency correction from the Tweeter to the Woofer. With this control scheme, the combination of a slow Woofer with a fast Tweeter has the same dynamic response as a single fast mirror. This allows for the large amplitude, low spatial frequency disturbances to be corrected by the Woofer without degrading the performance of the system. The measured Woofer Tweeter rejection ratios matched the rejection ratio expected from a fast single mirror system. The

bandwidth of this system is approximately 6.5% of the sample rate regardless of Woofer response speed. The computation cost of the proposed controller implementation increases linearly with the number of Tweeter actuators.

6. FUTURE WORK

Now that the basic components of the Woofer-Tweeter system are operational and behaving according to the expected models, the controller can be expanded to meet the needs of the TMT project. The mirrors should be upgraded to have actuator density on the same order as what would be used in a TMT instrument so that the desired amount of offloading can be verified. It is planned that a 1k actuator mirror will replace the 140 actuator Tweeter and a 9x9 Woofer to replace the 8x8 LAOG Woofer.

The initial TMT plans for the wave front reconstruction is a tomographic reconstruction followed by a filter given in Eq. 6.1 then given to a controller that is probably of the form given in Eq. 3.11. Rather than filter the error signal, then pass the result to the controller, the control approach provided in this paper performs both the filtering and the control at once using a specific case of $\alpha_0 = \alpha_1 = 0.5$ and $\beta_1 = \beta_2 = 0$. In other words, the closed loop response of the AO system will have the form given in Eq. 6.2, rather than using $f(z)$ as a sub component of the controller as shown in Eq. 6.3. This will accomplish the desired filtering of the WFS data prior to the mirror without excessive sacrifices to bandwidth. Note that the values of α and β are expected to be different depending if Eq. 6.2 or Eq. 6.3 is used. The control scheme for the general case of Eq. 6.1 has been developed but has yet to be experimentally tested. It is expected that allowing β to be non-zero would increase the computational complexity by 4n+8m, where n is Tweeter actuators and m is Woofer modes.

$$f(z) = \frac{\alpha_0 + \alpha_1 z^{-1}}{1 + \beta_1 z^{-1} + \beta_2 z^{-2}} \tag{6.1}$$

$$T_{current\ plan}(z) = f(z) G_{DM}(z) G_{WFS}(z) \tag{6.2}$$

$$T_{initial\ TMT\ plan}(z) = \frac{f(z) G_{CAO}(z) G_{DM}(z) G_{WFS}(z)}{1 + f(z) G_{CAO}(z) G_{DM}(z) G_{WFS}(z)} \tag{6.3}$$

It is understood that the plan for TMT is to combine several NGS wave front error measurements to determine the necessary tilt and focus correction. The controller will be expanded to allow for multiple sources of wave front data for these 3 low order modes.

REFERENCES

1. Tyson, R.K., *Introduction to Adaptive Optics*, SPIE Press, Bellingham, Washington, 2000.
2. Noll, R.L., Zernike Polynomials and Atmospheric Turbulence, J. Optical Society of America, 207-211, 1976.
3. Hampton, P.J., Design and Implementation of Discrete Type 1 and Type 2 Controllers with Residual Feedback for Modal Adaptive Optics, M.Sc. Thesis, University of Victoria, Victoria, BC, 2005.
4. Ogata, K., *Discrete-Time Control Systems, Second Edition*, Prentice-Hall, Inc., New Jersey, USA, 1995.
5. Watkins, D.S., *Fundamentals of Matrix Computations*, John Wiley & Sons, Inc., New York, USA, 2002.